nature cell biology

DOI: 10.1038/ncb3369

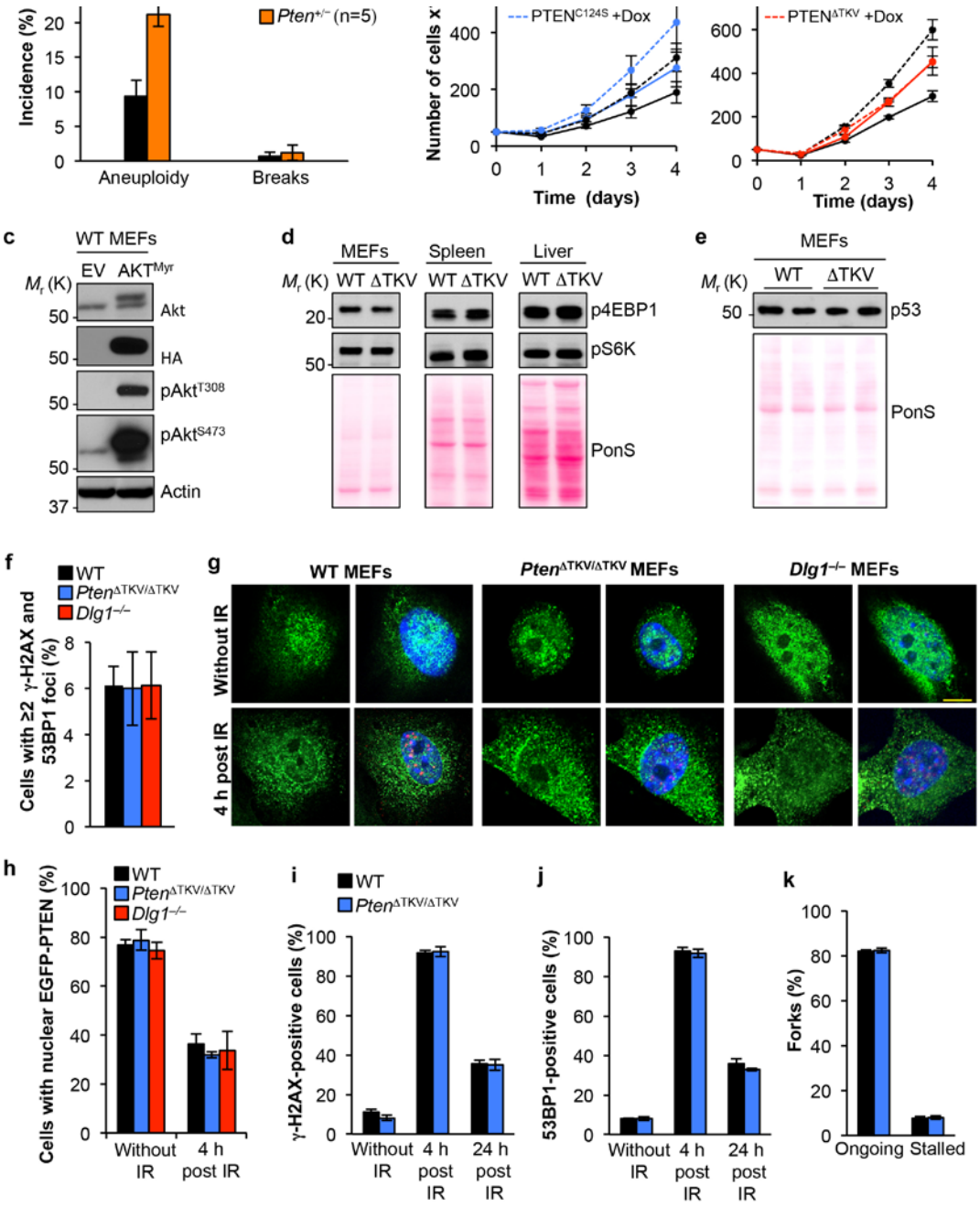

Supplementary Figure 1 Akt signaling and structural chromosome integrity seems unaffected by PDZ-BD loss. **(a)** Analysis of metaphase spreads from P5 MEFs for abnormal chromosome numbers and DSBs. n = the number of independent MEF lines (50 and 100 spreads per line were analyzed for assessments of aneuploidy and chromosome breaks, respectively). **(b)** Growth curves of induced and non-induced MEFs containing the indicated Pten expression constructs. n = 3 independent MEF lines for each growth curve. Note that induction of ectopic expression of WT or mutant PTEN proteins had no negative impact on cell proliferation. (**c**) Western blots of lysates from WT MEFs carrying HA-tagged AKT^{Myr} introduced by a lentiviral expression vector (EV, empty vector). **(d)** Western blots of lysates from WT and *Pten*$^{\Delta TKV/\Delta TKV}$ MEFs, spleens and livers. Pon S staining of blotted proteins served as a loading control. **(e)** Western blot of asynchronous MEF extracts. Pon S staining served as a loading control. (**f**) Incidence of MEFs with ≥ 2 γ-H2AX/53BP1-positive foci. n = 3 independent MEF lines (n = 500 cells per line). **(g)** EGFP-PTEN localization in MEFs prior to and 4 h after 5 Gy γ-irradiation. γ-H2AX (in red) co-staining was used as a marker for DNA damage. Bar, 5 μm. **(h)** Quantitation of MEFs with nuclear EGFP-PTEN localization prior to and 4 h after γ- irradiation. n = 3 independent MEF lines. **(i** and **j)** Analysis of DSB repair following 5 Gy γ-irradiation using γ-H2AX and 53BP1 as DSB markers. Quantification was done on n = 3 independent MEF lines (119-191 cells per line). **(k)** Analysis of DNA replication efficiency using DNA fiber assays. This analysis was carried out on n = 3 independent MEF lines (102-202 replication forks per line). Data in **b** and **h-k** represent mean ± s.e.m., and in **a** and **f** mean ± s.d. Statistical significance was determined by a two-tailed unpaired t-test. ***, $P<0.001$. Unprocessed original scans of blots can be found in Supplementary Fig. 6 and Statistics Source Data in Supplementary Table 1.

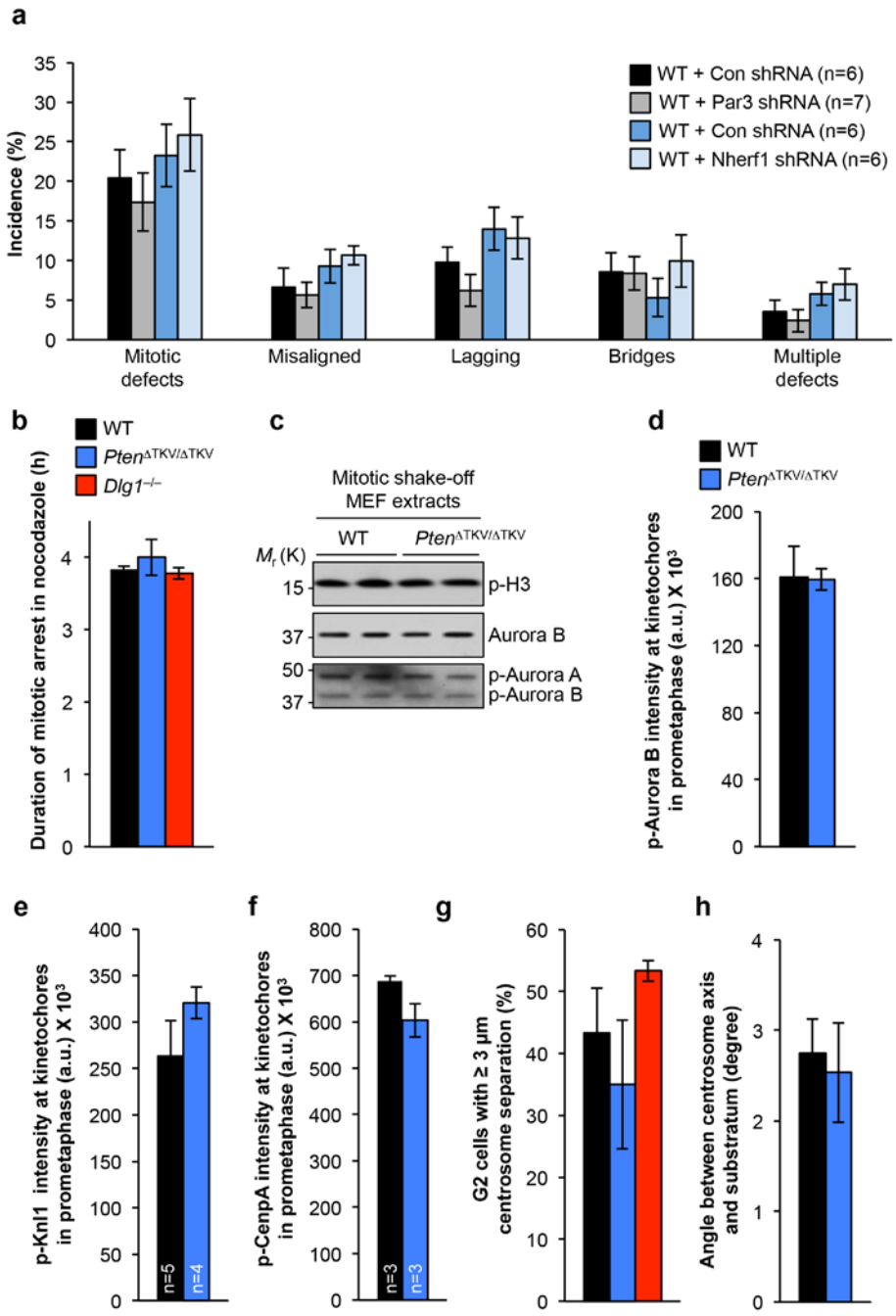

Supplementary Figure 2 Mitotic surveillance mechanisms are not affected in *Pten*$^{\Delta TKV/\Delta TKV}$ MEFs. **(a)** WT MEFs with or without knockdown of Par3 or Nherf1 monitored for mitotic defects by live-cell imaging as they progress through mitosis. n = the number of independent experiments (≥ 24 cells per line). **(b)** Spindle assembly checkpoint analysis by standard nocodazole-challenge assay. Mitotic arrest duration of *Pten*$^{\Delta TKV/\Delta TKV}$ and *Dlg1*$^{-/-}$ MEFs after nocodazole addition. n = 3 MEF lines per genotype (8-26 cells per line). **(c-f)** Error correction machinery analysis in *Pten*$^{\Delta TKV/\Delta TKV}$ MEFs. **(c)** Western blot analysis of mitotic lysates of WT and *Pten*$^{\Delta TKV/\Delta TKV}$ MEFs immunoblotted for Aurora B and p-Aurora, demonstrating that this core component of this machinery was normally expressed and activated in mitosis. P-histone H3 (p-H3) served as a control for equal loading of mitotic cells. **(d)** Quantitation of p-Aurora B kinase signals at inner centromeres in prometaphase MEFs, demonstrating proper Aurora B in *Pten*$^{\Delta TKV/\Delta TKV}$ MEFs. n = 3 independent cell lines (10 cells per line) **(e** and **f)** Quantitation of two key kinetochore-associated substrates of Aurora B, p-Knl1 **(e)** and p-CenpA **(f)**, further indicating that error correction was normal in cells lacking the Pten PDZ-BD. n = the number of independent MEF lines (12-20 cells per line) **(g)** Incidence of MEFs with centrosome distance ≥ 3 µm in G2 as a measure for early centrosome separation. Costaining with p-Histone H3 served to identify cells in G2 phase. n = 3 independent MEF lines (20 cells per line). **(h)** Analysis of planar spindle orientation. n = 3 independent MEF lines (10 cells per line). Data in **a**, **d**-**h** represent mean ± s.e.m. and in **b** represent mean ± s.d. Statistical significance was determined by a two-tailed unpaired t-test. Unprocessed original scans of blots can be found in Supplementary Fig. 6 and Statistics Source Data in Supplementary Table 1.

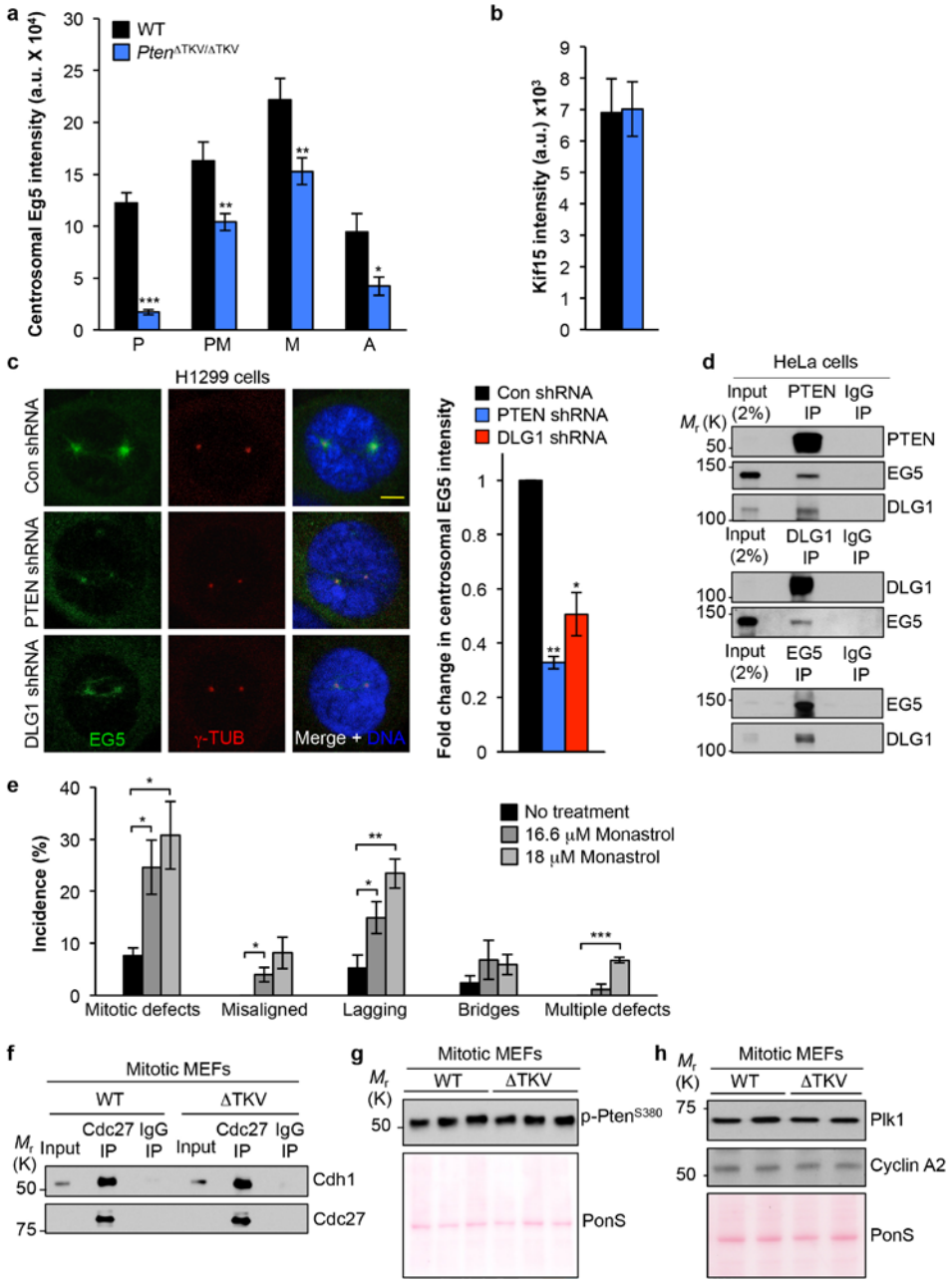

Supplementary Figure 3 WT MEFs subjected to partial Eg5 inhibition have similar chromosome segregation errors as *Pten*$^{\Delta TKV/\Delta TKV}$ and *Dlg1*$^{-/-}$ MEFs. **(a)** Quantification of Eg5 signal at astral microtubules and centrosomes at various mitotic stages. n = 15 MEFs per mitotic stage per genotype. **(b)** Quantitation of Kif15 signals at centrosomes. The analysis was done on n=3 independent MEF lines per genotype (5 cells per line). **(c)** Images of HT1299 prophase cells immunostained for EG5 and γ-tubulin 72 h after transduction with the indicated shRNA lentiviruses (bar, 5 μm). Quantitation of EG5 signals at centrosomes for n = 3 independent immunostaining experiments (10-15 cells per experiment). **(d)** Analysis of complex formation between endogenous PTEN, DLG1 and EG5 in mitotic HeLa cells by reciprocal co-immunoprecipitation assays. Blots are representative of 2 independent experiments. **(e)** WT MEFs treated with indicated amount of monastrol monitored for mitotic defects by live-cell imaging as they progress through mitosis. The analysis was performed on n = 5 independent MEF lines (>13-37 cells per line). **(f-h)** APC/C^{Cdh1} assembly is unperturbed in *Pten*$^{\Delta TKV/\Delta TKV}$ cells. **(f)** Immunoblots of mitotic WT and *Pten*$^{\Delta TKV/\Delta TKV}$ MEF lysates subjected to immunoprecipitation with Cdc27 or control (IgG) antibodies and analyzed by western blotting with Cdh1 and Cdc27 antibodies. Blots are representative for 3 independent experiments. **(g)** Western blot analysis of mitotic MEF lysates for p-Pten^{S380}. Phosphorylation of S380 by Plk1 during mitosis controls Pten association with Cdh1[18]: this regulatory mechanism is unperturbed when the Pten PDZ-BD is lacking. **(h)** Western blot analysis of mitotic lysates of WT and *Pten*$^{\Delta TKV/\Delta TKV}$ MEFs for select mitotic substrates that are subject to degradation by APC/C^{Cdh1}. Pon S staining of blotted proteins served as a loading control. Data in **a-c**, **e** represent mean ± s.e.m. Statistical significance in **a** and **b** was determined by a two-tailed unpaired *t*-test, in **c** by a one-sample *t*-test against a theoretical mean of unity, and in **e** by a two-tailed paired *t*-test. * $p < 0.05$, ** $p < 0.01$, *** $p < 0.001$. Unprocessed original scans of blots can be found in Supplementary Fig. 6 and Statistics Source Data in Supplementary Table 1.

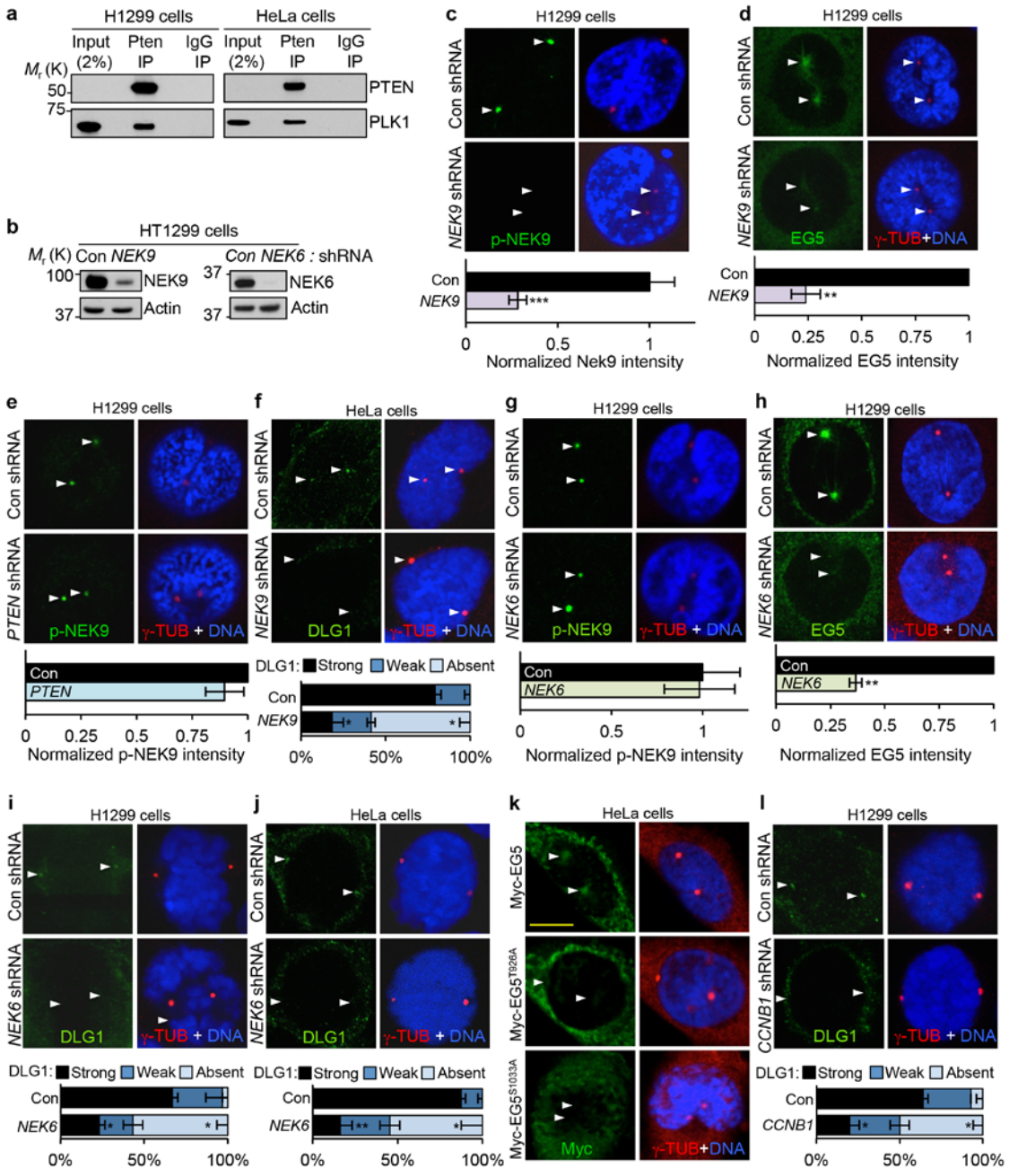

Supplementary Figure 4 DLG1-mediated docking of EG5 to PTEN at centrosomes is dependent on NEK9-NEK6 and cyclin B1-CDK1 kinase activity. **(a)** Immunoblots of mitotic HT1299 or HeLa extracts subjected to immunoprecipitation with PTEN antibody or control IgG and analyzed with the indicated antibodies. Blots are representative for 2 independent experiments. **(b)** Western blots of lysates from HT1299 cells transduced with *NEK6* or *NEK9* shRNA or non-silencing shRNA negative control (Con) lentiviruses and analyzed 72 h later. **(c)** Prophase cells stained for p-NEK9^{T210} after transduction with *NEK9* shRNA or non-silencing control shRNA. Centrosome-associated p-NEK9^{T210} was quantified. **(d)** As **c** stained for EG5. Centrosome-associated EG5 was quantified. **(e)** Prophase cells stained for p-NEK9^{T210} after transduction with *PTEN* shRNA or non-silencing control shRNA. Centrosome-associated p-NEK9^{T210} was quantified. **(f)** As **c** stained for DLG1. Centrosome-associated DLG1 was quantified. **(g)** Prophase cells stained for p-NEK9^{T210} after transduction with *NEK6* shRNA or non-silencing control shRNA. Centrosome-associated p-NEK9^{T210} was quantified. **(h)** As **g** stained for EG5. Centrosome-associated EG5 was quantified. **(i** and **j)** As **g** stained for DLG1. Centrosome-associated DLG1 was quantified. **(k)** Prophase cells transiently expressing Myc-tagged WT or mutant EG5 immunostained for ectopic EG5. **(l)** As **i** but for prophase cells depleted for *CCNB1*. All data presented are mean ± s.e.m. n = 3 independent experiments in **d-f**, **h-j** and **l** (10-18 cells per condition) and n = 10 cells in **c** and **g**. Statistical significance in **d, e** and **h** was determined by a one-sample *t*-test against a theoretical mean of unity, in **c** and **g** by an unpaired *t*-test and in **f**, **i**, **j** and **l** by a two-tailed paired *t*-test. * $p < 0.05$, ** $p < 0.01$, *** $p < 0.001$. Unprocessed original scans of blots can be found in Supplementary Fig. 6 and Statistics Source Data in Supplementary Table 1.

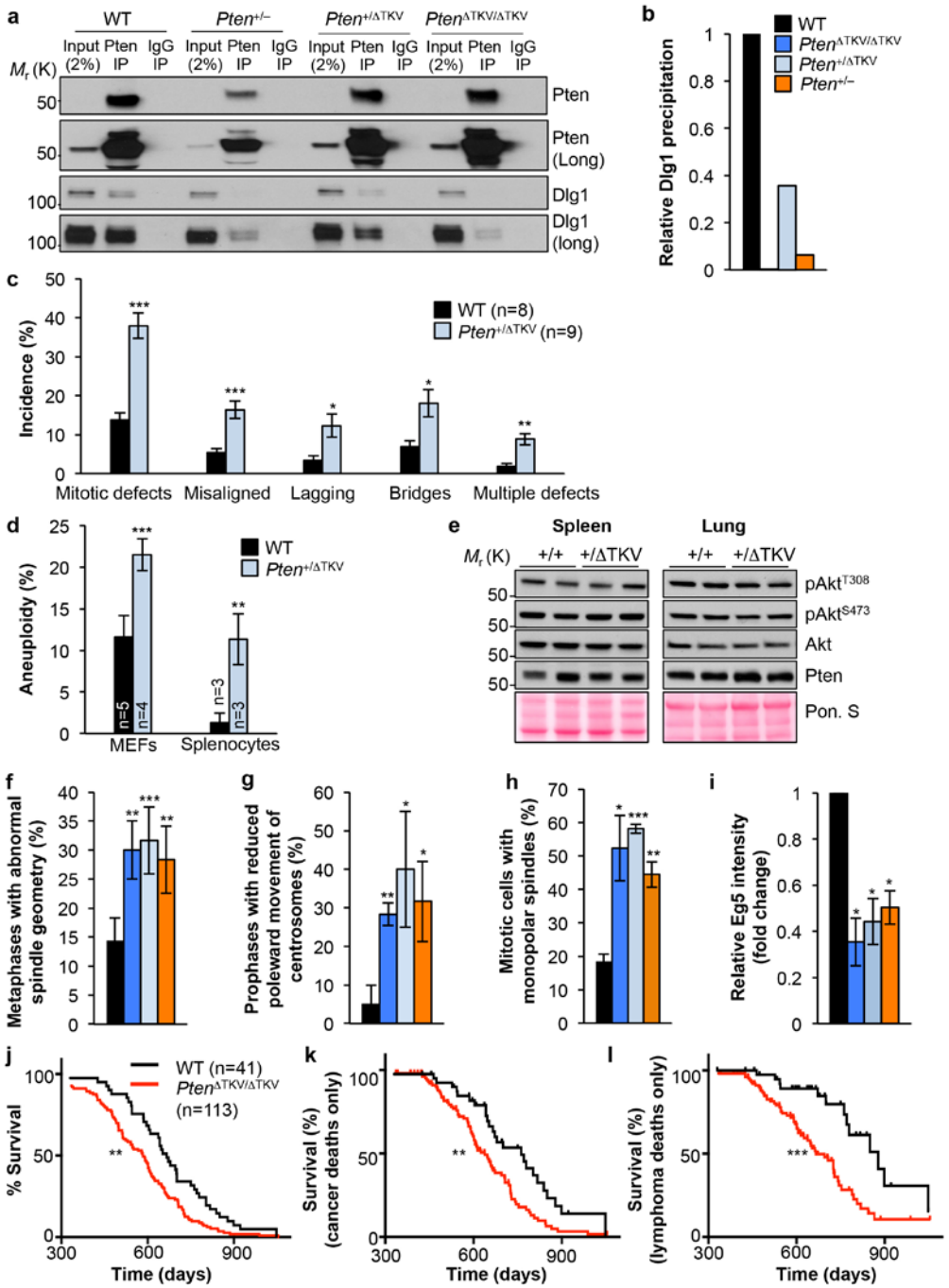

Supplementary Figure 5 Partial Pten PDZ-BD loss perturbs spindle assembly and cause chromosome missegregation. **(a)** Immunoblots of mitotic MEF extracts precipitated with indicated antibodies and analyzed for Dlg1 (representative for 2 experiments). **(b)** Relative Pten-Dlg1 complex formation (mean of 2 independent experiments). **(c)** MEFs analyzed for mitotic defects. n = the number of independent MEF lines (29-71 cells/line). **(d)** Karyotyping of MEFs and splenocytes from 5-month-old mice. n = the number of independent MEF lines or spleens (50 spreads/MEF line or spleen). **(e)** Western blots of lysates from indicated tissues of WT and $Pten^{+/\Delta TKV}$ mice. **(f)** Incidence of spindle asymmetry. n = the number of independent MEF lines (20 cells/line). **(g)** Incidence of prophases with reduced centrosome movement. n=3 independent MEF lines (20 cells/line). **(h)** Monopolar spindle formation in 16.6 µM monastrol. n=3 independent MEF lines (64-95 cells/line). **(i)** Quantification of Eg5 signal at astral microtubules and centrosomes in prophase. n=3 independent MEF lines/genotype (10 cells/line). **(j)** Overall survival curves showing that $Pten^{\Delta TKV/\Delta TKV}$ lifespan is shortened. **(k)** Survival curves of WT and $Pten^{\Delta TKV/\Delta TKV}$ mice dying with tumors showing that $Pten^{\Delta TKV/\Delta TKV}$ mice develop tumors faster, although the overall tumor incidence was unchanged (66% in WT versus 67% in $Pten^{\Delta TKV/\Delta TKV}$ mice). The tumor spectrum of both WT and $Pten^{\Delta TKV/\Delta TKV}$ mice consisted of lymphomas, sarcomas, and liver and lung tumors. Of these, the incidence of lymphomas was significantly increased in $Pten^{\Delta TKV/\Delta TKV}$ mice (50% versus 32% in WT mice). **(l)** Survival curves of mice dying with lymphoma showing that lymphomas are not only more prevalent in $Pten^{\Delta TKV/\Delta TKV}$ mice, but also develop faster. WT and $Pten^{\Delta TKV/\Delta TKV}$ values in **f** and **g** were taken from Fig. 2f, h. Data shown in **b**, **d**, **f** and **g** are the mean ± s.d., in **c**, **h** and **i** the mean ± s.e.m. Statistical significance in **c, d, f-h** was determined by unpaired *t*-test, and in **b**, **i** by a one-sample *t*-test against a theoretical mean of unity, and by Log-rank tests in **j-l**. * $p < 0.05$, ** $p < 0.01$, *** $p < 0.001$. See Supplementary Fig. 6 for unprocessed blot scans and Supplementary Table 1 for Statistics Source Data.

Un-cropped blots Fig. 1d

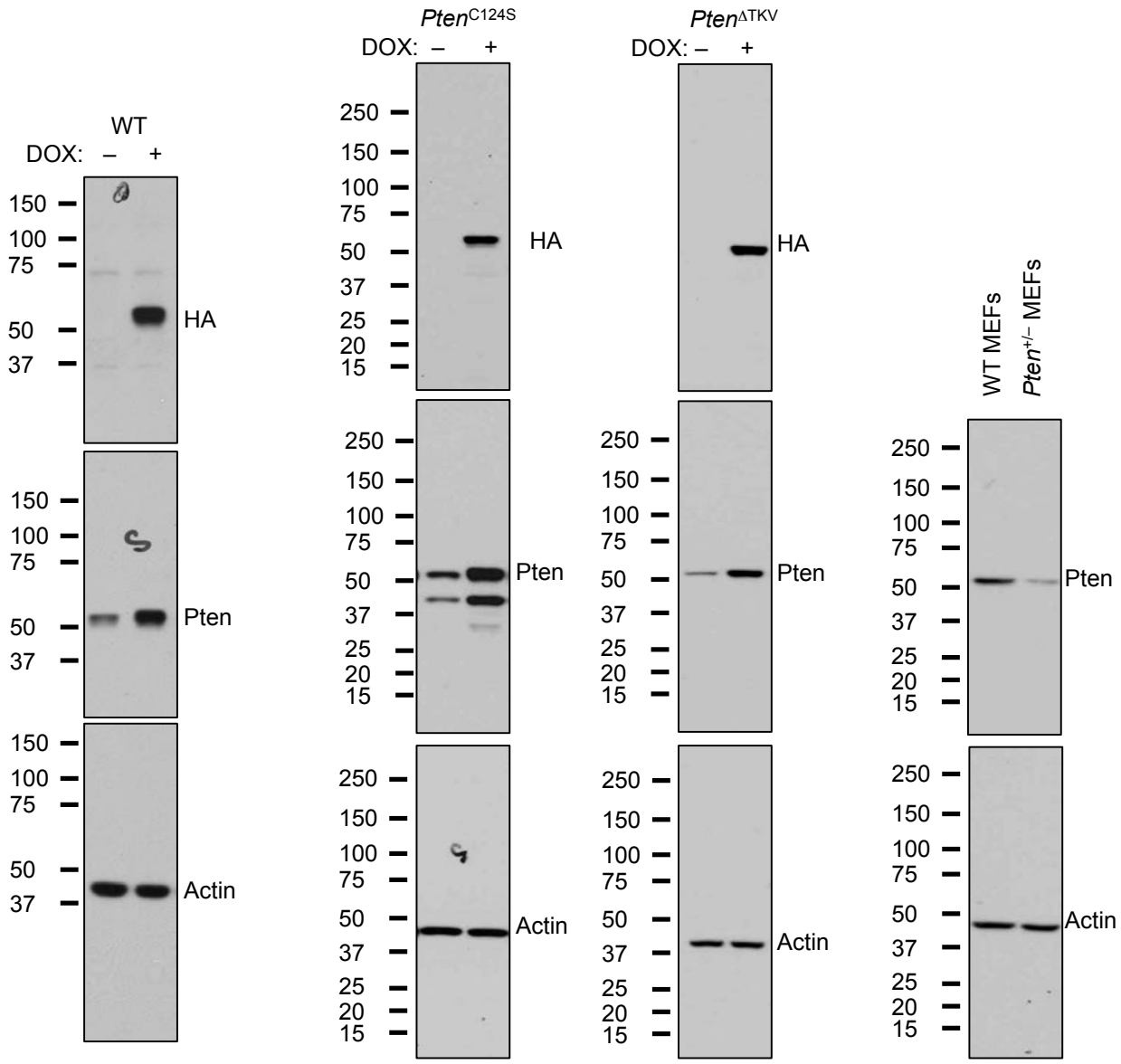

Supplementary Figure 6 Unprocessed scans of blots

Un-cropped blots Fig. 1f

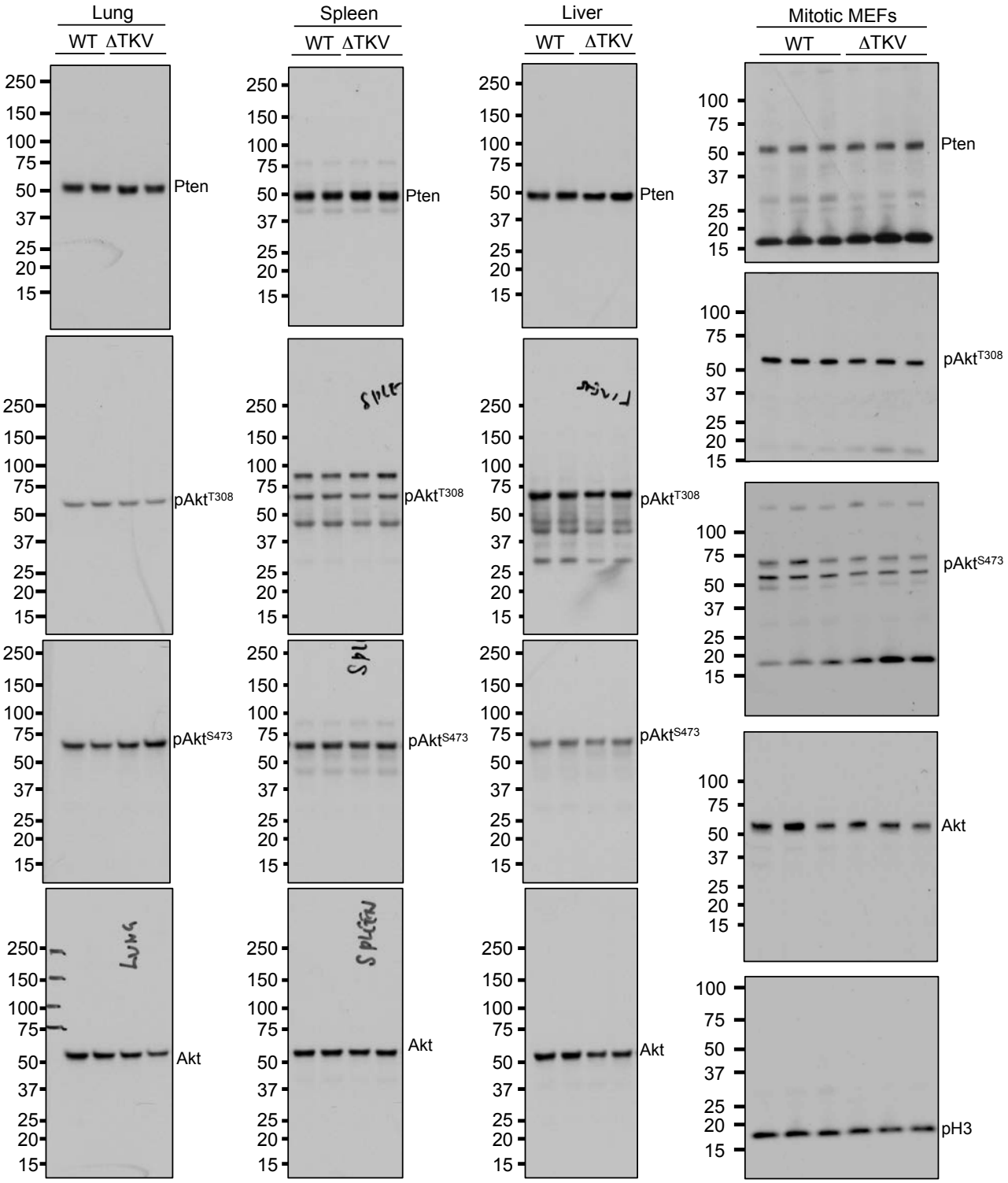

Supplementary Figure 6 Unprocessed scans of blots

Un-cropped blots Fig. 2a and d

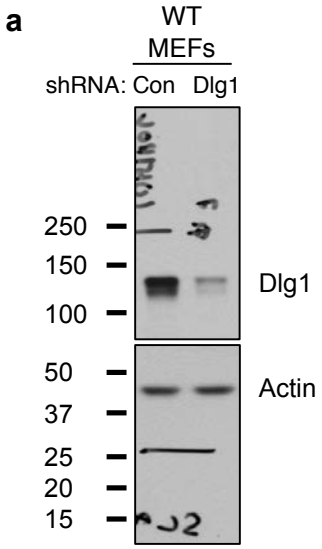

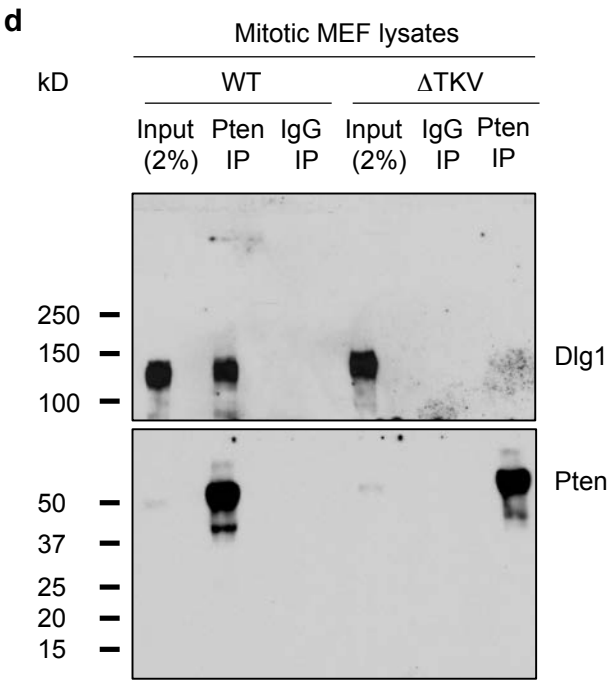

Supplementary Figure 6 continued

Un-cropped blots Fig. 3f

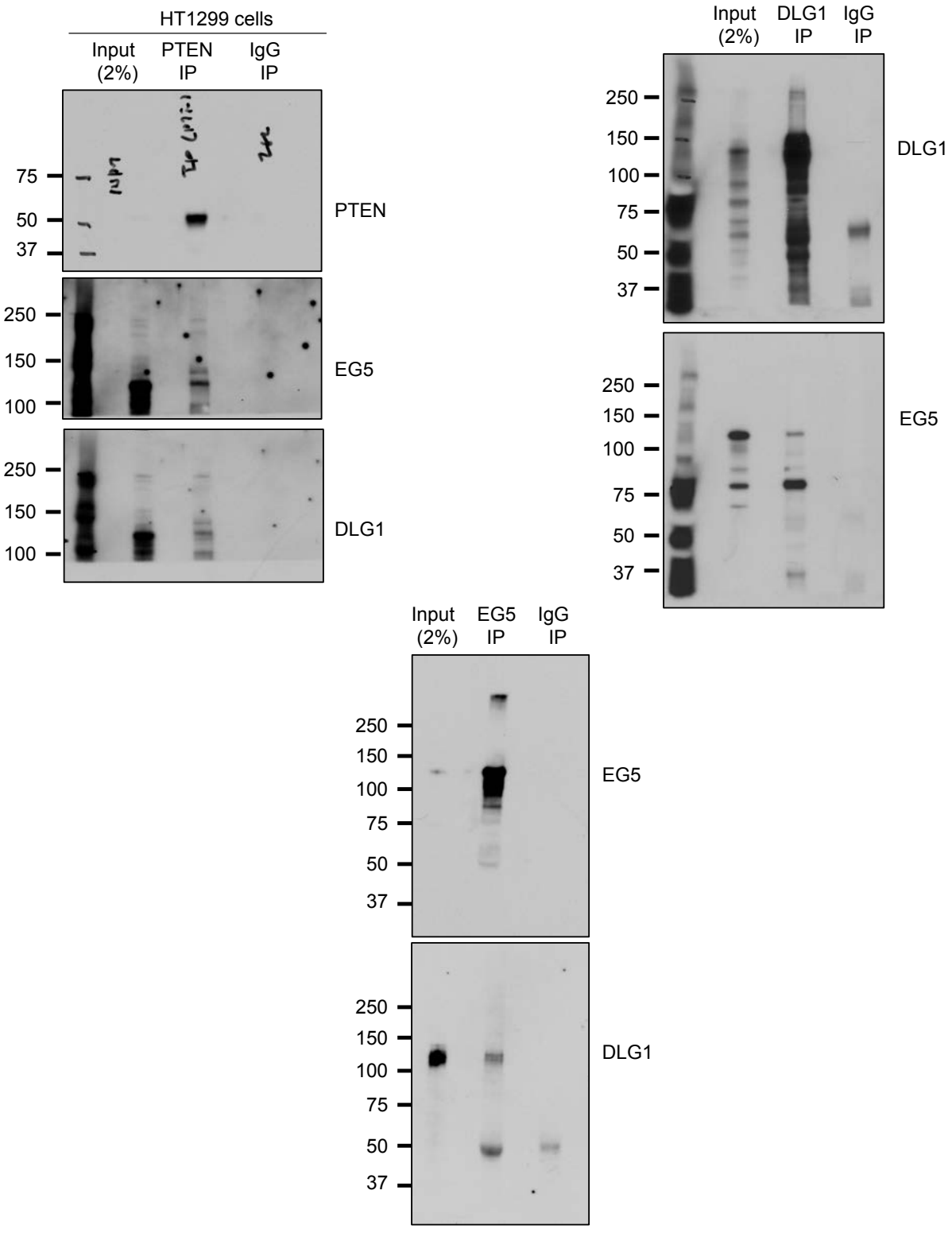

Supplementary Figure 6 continued

Un-cropped blots Fig. 3g and h

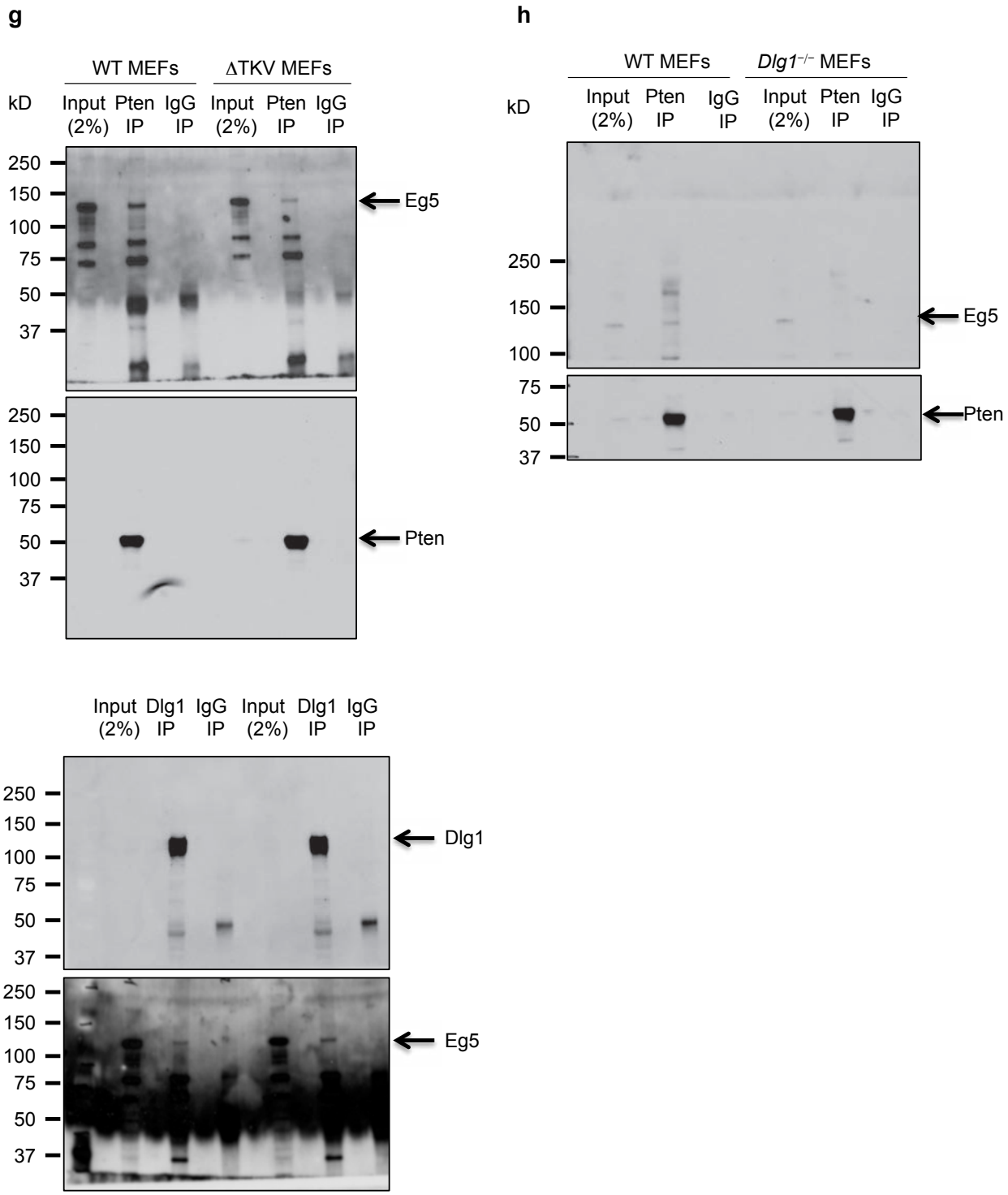

Supplementary Figure 6 continued

Un-cropped blots Fig. 4e and j

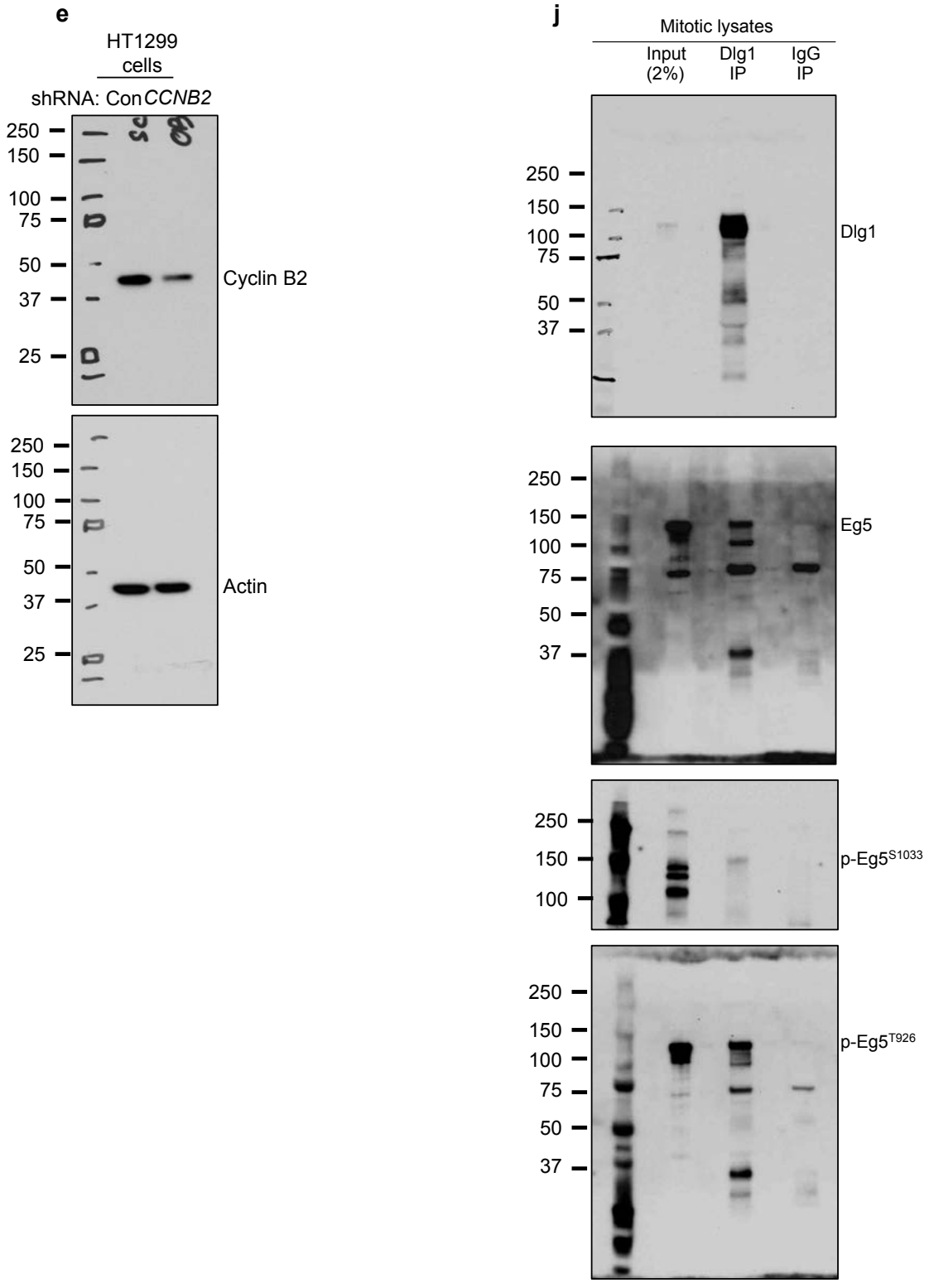

Supplementary Figure 6 continued

Un-cropped blots Fig. 4k

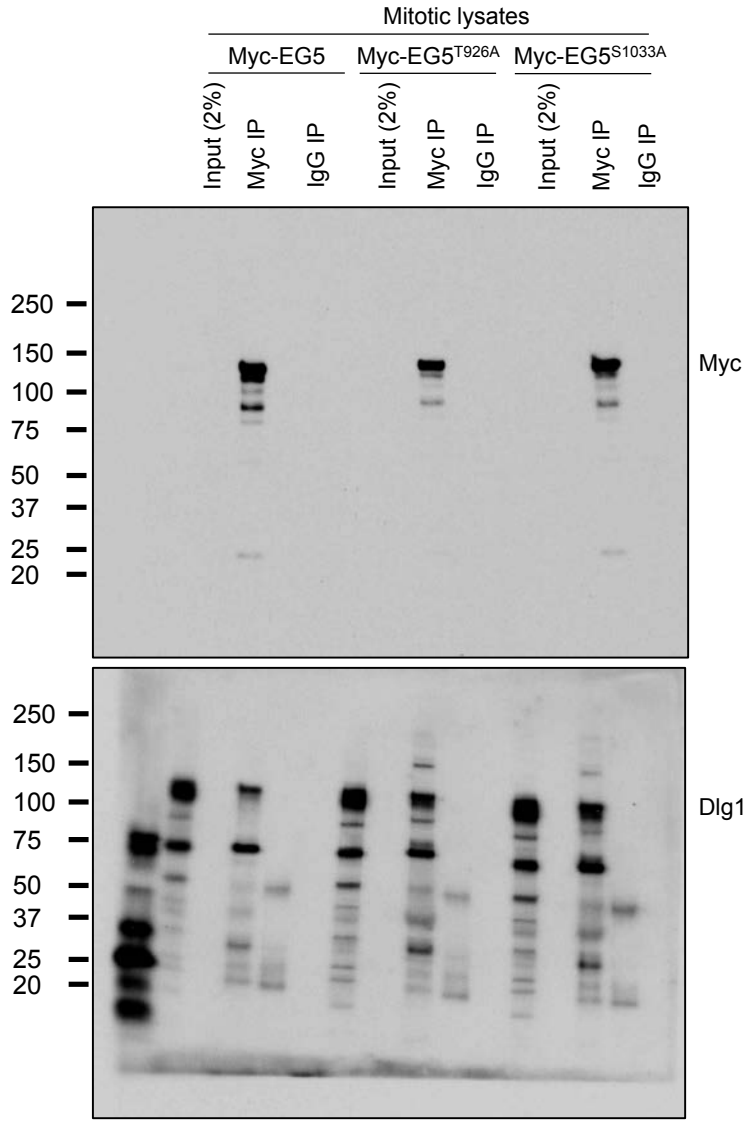

Supplementary Figure 6 continued

Un-cropped blots Fig. 5f

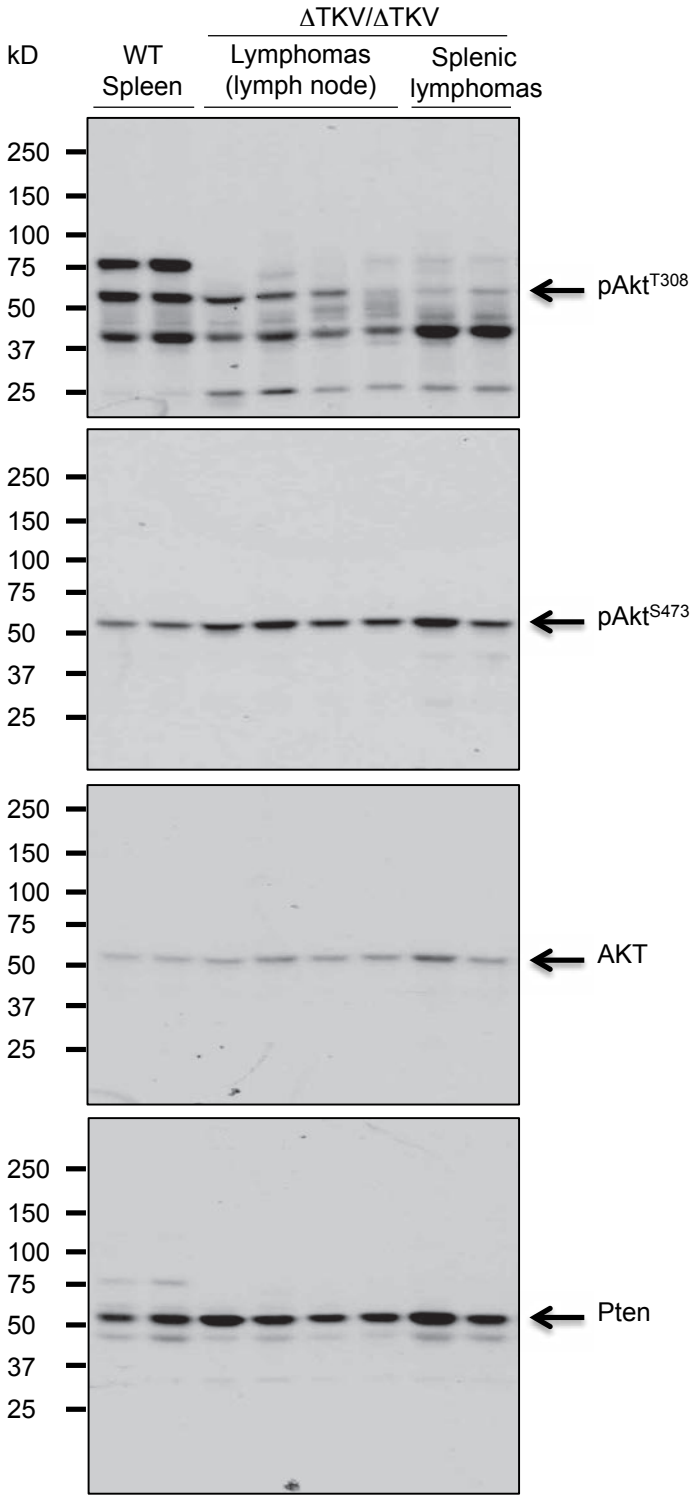

Supplementary Figure 6 continued

Un-cropped blots Supplementary Fig. 1c-e

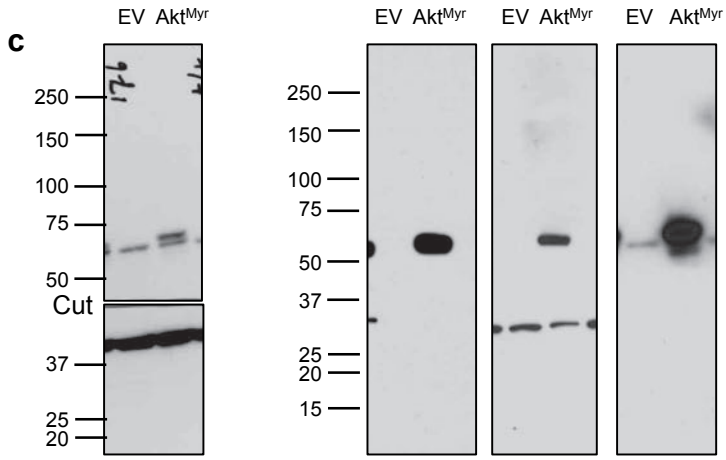

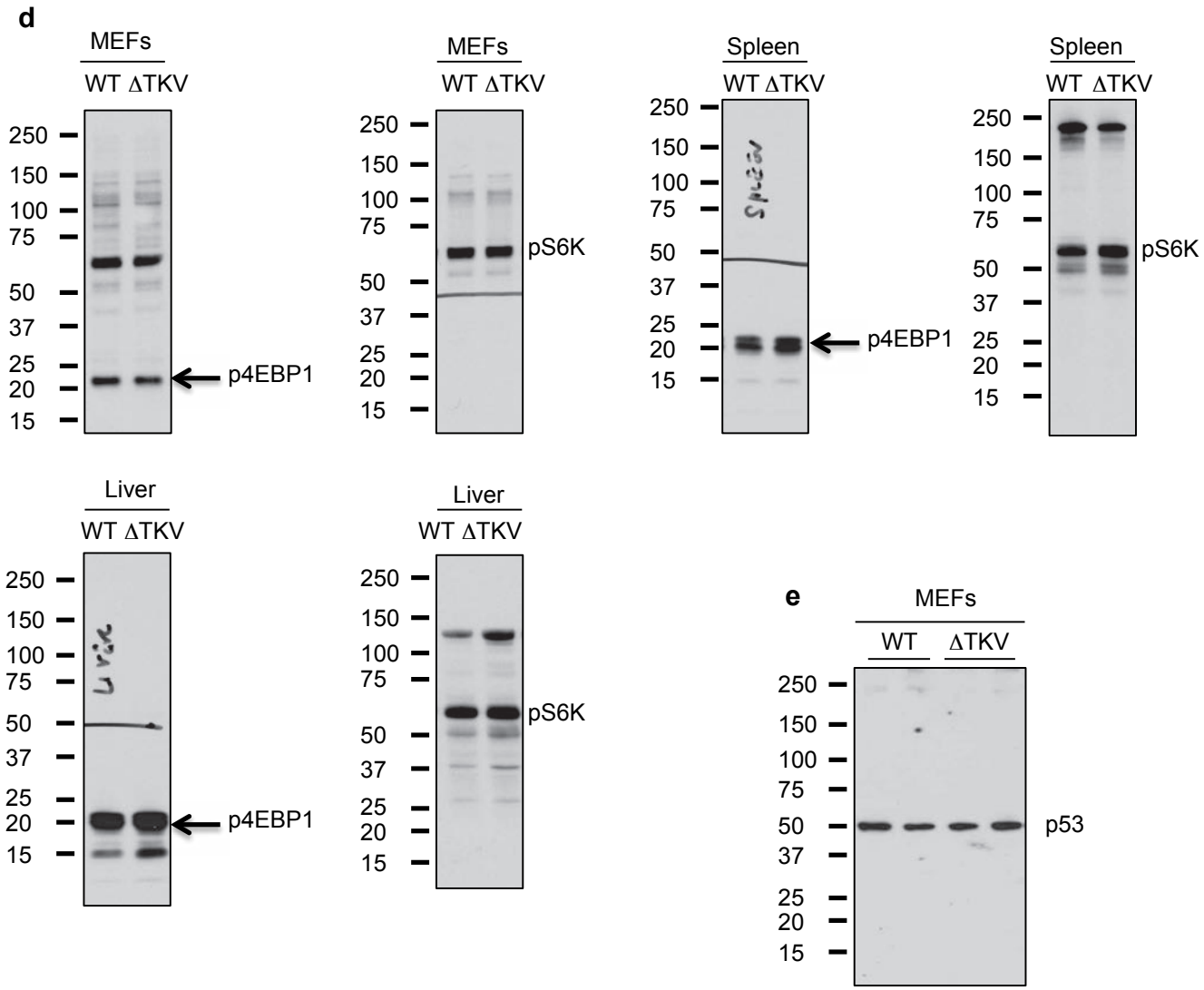

Supplementary Figure 6 continued

Un-cropped blots Supplementary Fig. 2c

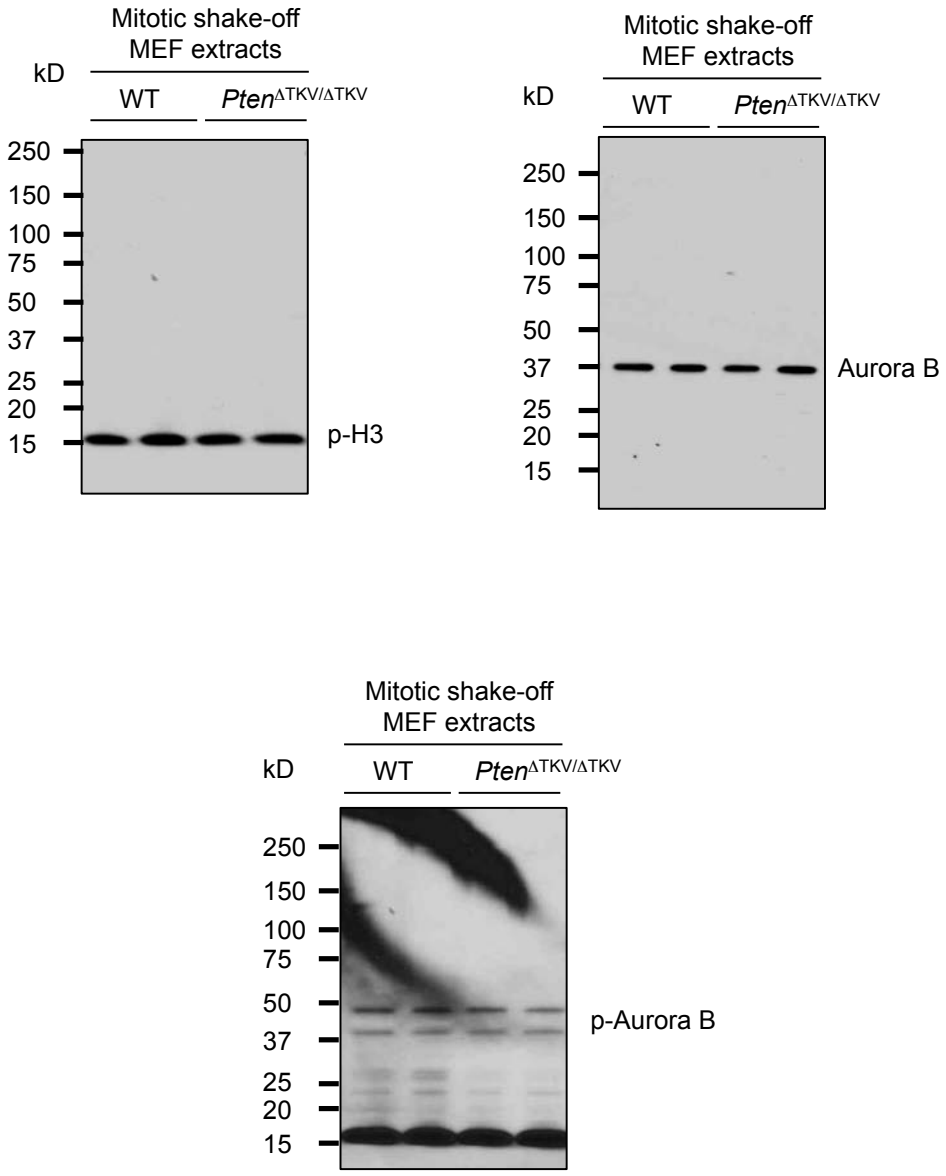

Supplementary Figure 6 continued

Un-cropped blots Supplementary Fig. 3b

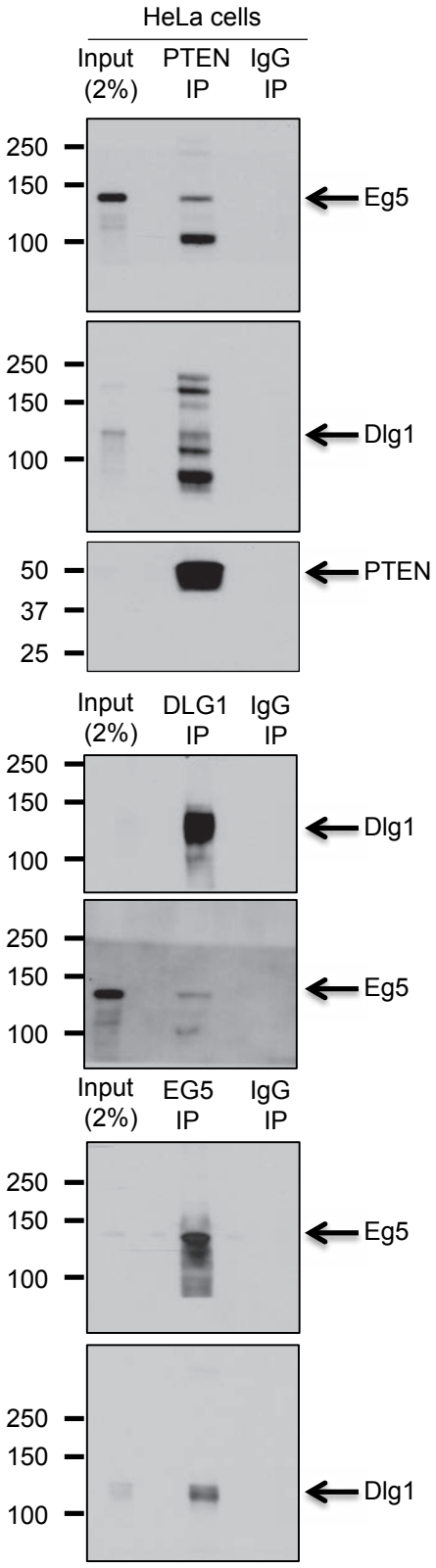

Supplementary Figure 6 continued

Un-cropped blots Supplementary Fig. 3d-f

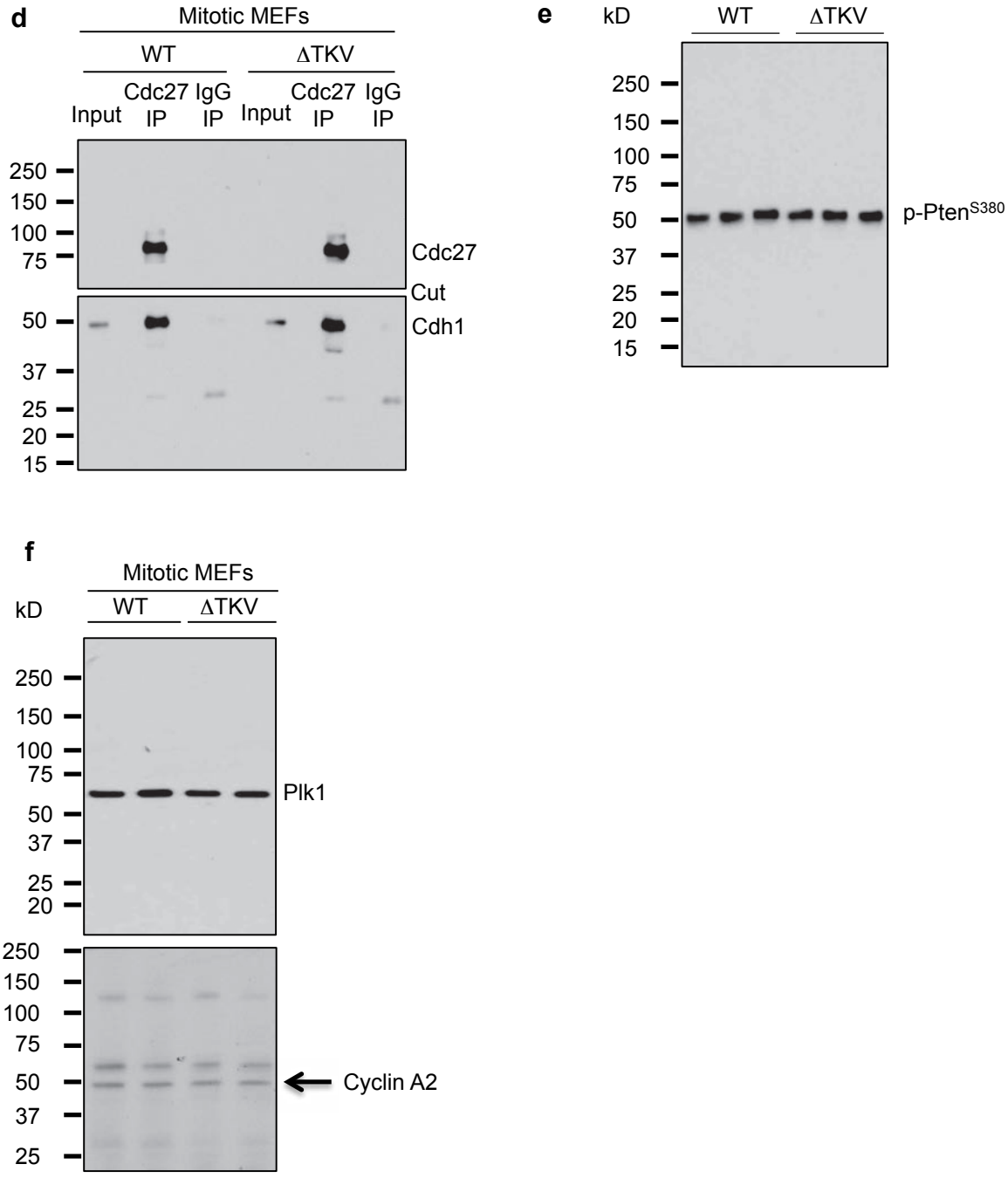

Supplementary Figure 6 continued

Un-cropped blots Supplementary Fig. 4a and b

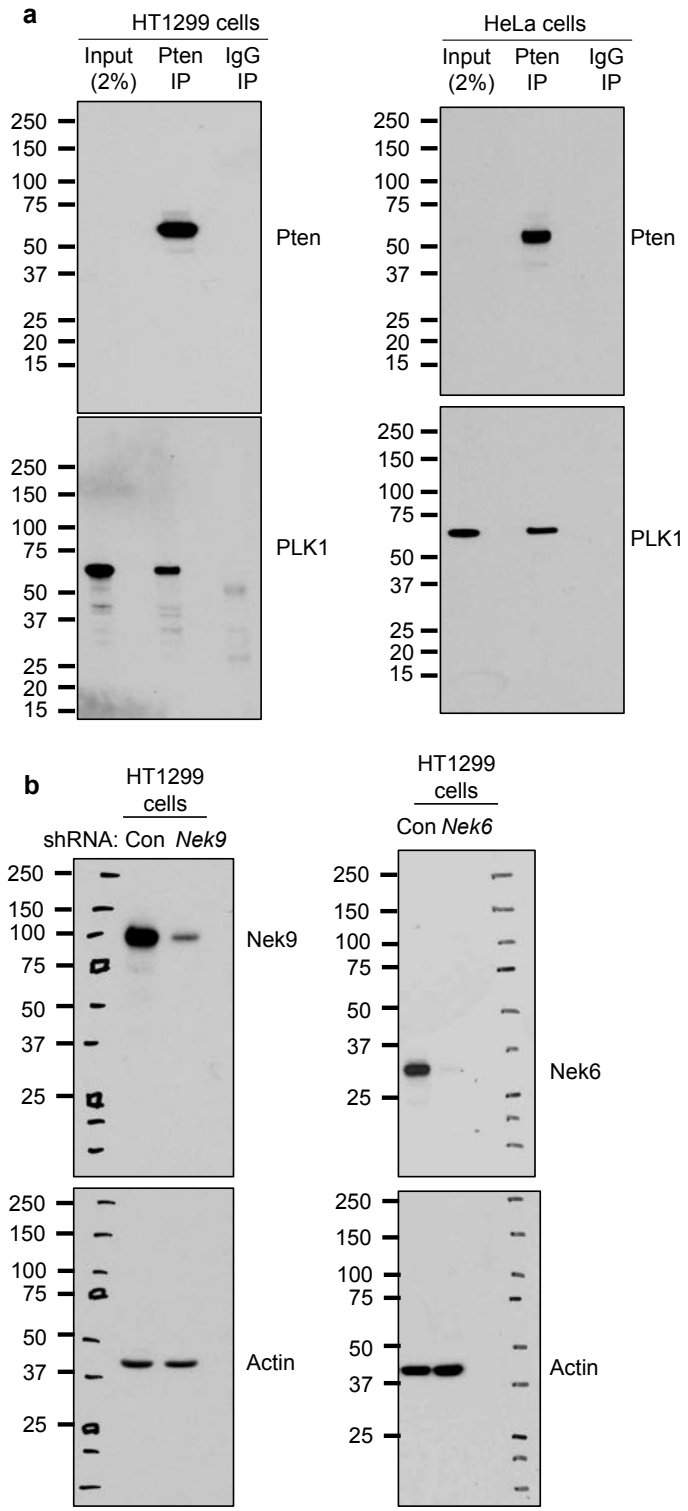

Supplementary Figure 6 continued

Un-cropped blots Supplementary Fig. 5a

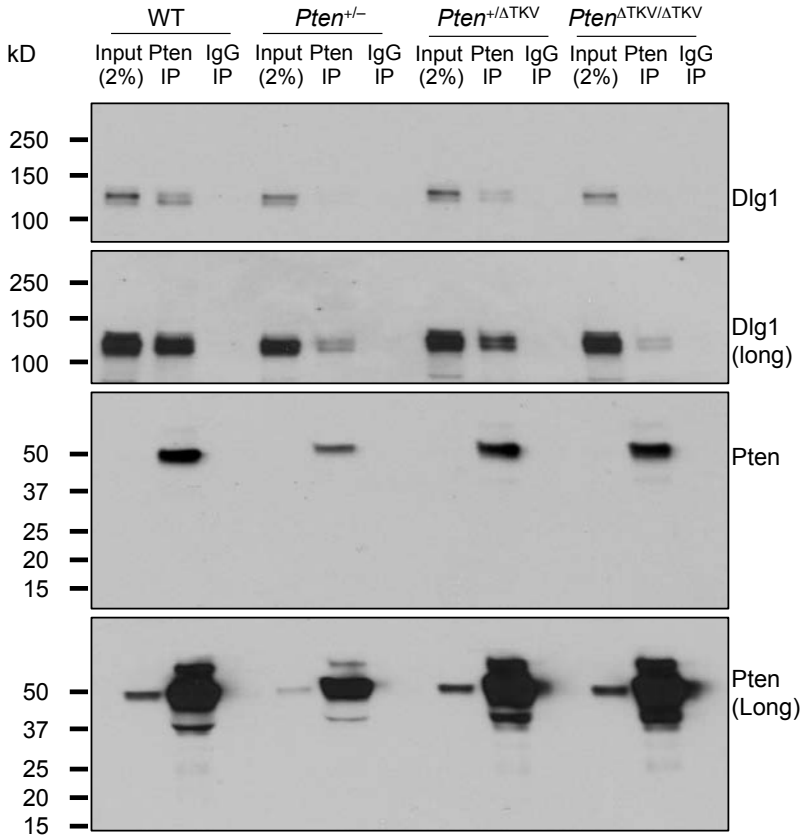

Supplementary Figure 6 continued

Un-cropped blots Supplementary Fig. 5e

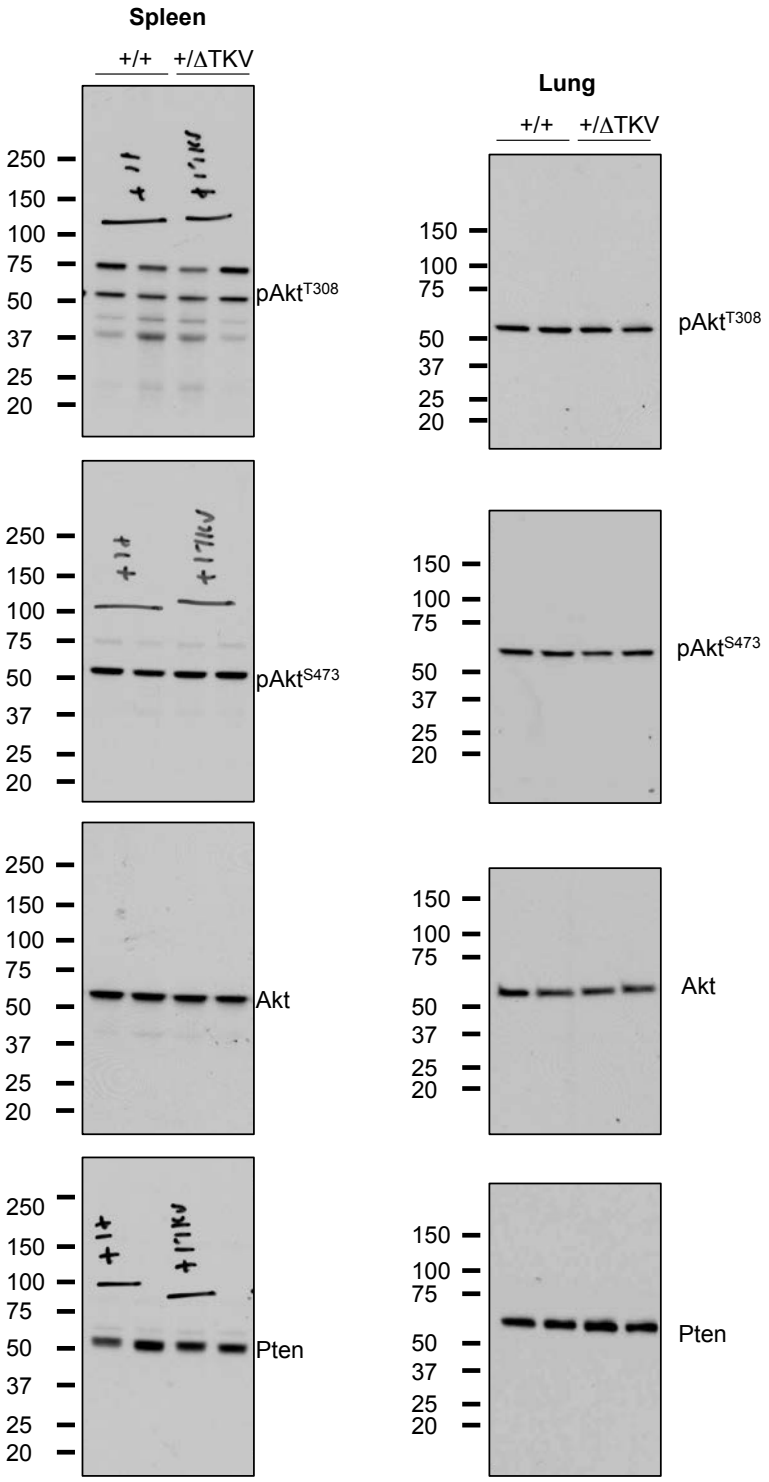

Supplementary Figure 6 continued

Supplementary Table 1 Statistics Source data